Computers Chem. Vol. 17, No. 1, pp. 91–102, 1993
Printed in Great Britain.

0097-8485/93 $6.00 + 0.00

TESTS ON COMBINED PROJECTION/FORWARD DIFFERENCING INTEGRATION FOR STIFF PHOTOCHEMICAL FAMILY SYSTEMS AT LONG TIME STEP

SCOTT ELLIOTT,* RICHARD P. TURCO and MARK Z. JACOBSON
Department of Atmospheric Sciences, University of California, Los Angeles, CA 90024, U.S.A.

(Received 28 August 1991; in revised form 10 August 1992)

Abstract—Accurate estimates of final tracer concentrations guide adjustment of individual species levels so that forward integration of stiff families can proceed at time steps an order of magnitude larger than inherent loss constants. Maintenance of a unified concentration vector in the solver ensures mass conservation. The sequence was perfected by raising the step size upward from 100 s in a standard 25 family 45 species stratospheric box model with explicit Euler numerics. Projections were inserted as instabilities arose. Ultimately, a uniform Δt of 1 h was achieved from 20–50 km at mid-latitudes. Results were compared over five equinoctial diurnal cycles with runs at 0.1 and 1 s steps in which every constituent other than the individual atoms, CHO and CH_3O, was handled separately. Agreement was better than 10^{-2} for the major reservoirs in almost all cases, and was equally close for radicals between 6 a.m. and 6 p.m., provided that photolysis constants were time averaged. The few exceptions were due to experimentation with a linearized implicit concentration predictor, or to the approximations underlying family partitioning recipes. CPU timings extrapolated to a hypothetical GCM grid suggest that 3-D modeling will be possible at the level of chemical resolution in the programs.

INTRODUCTION

Simulation of the interplay between photochemistry and fluid dynamics offers a continuing challenge in the environmental and combustion sciences (Oran & Boris, 1981; Garcia & Solomon, 1983; Carmichael *et al.*, 1986), and many other fields as well (e.g. Reinhardt, 1977). Consideration of all three physical dimensions is required for adequate treatment of many pressing problems, particularly those pertaining to the global atmosphere (Kaye & Rood, 1989; Rose & Brasseur, 1989; Brasseur *et al.*, 1990), but chemical kinetics are computationally stressful on finer grids (McRae *et al.*, 1982). Photochemical systems in the general circulation model (GCM) framework, for example, have often been restricted to small numbers of tracers (Cunnold *et al.*, 1975; Mahlman & Moxim, 1978; Prather *et al.*, 1987), and production and loss are sometimes parameterized off line (Jacob *et al.*, 1989; Spivakovsky *et al.*, 1990; Dunker, 1986; Marsden *et al.*, 1987).

A significant portion of the difficulty in merging chemistry with dynamics is attributable to the stiffness phenomenon. Numerous sophisticated integration techniques have been suggested to deal with stiff chemical equations in transport codes. Packaged integrators such as the Gear routine (Gear, 1969; Edelson, 1976; Weigert, 1987) were incorporated in early low dimensionality atmospheric models, but despite the higher speeds attainable in contemporary supercomputing, they are now thought to be overly expensive (McRae *et al.*, 1982; Kasting *et al.*, 1984; Chang *et al.*, 1987). Implicit differencing functions at large step sizes, but yields operation intensive coupled algebra (Wofsy, 1978; Logan *et al.*, 1978; McRae *et al.*, 1982). Collection of rapidly interchanging species into families both increases the permissible time step and reduces the total tracer number (Chapman, 1930; Crutzen, 1971; Brasseur & Solomon, 1984; Shimazaki, 1985). The family method has enabled the insertion of relatively detailed chemistry in several three-dimensional studies (Rose & Brasseur, 1989; Kao *et al.*, 1990). Even so, the extra grouping entailed has meant a loss of traditional reservoirs, and so also of maternal resolution (Douglass *et al.*, 1989; Brasseur *et al.*, 1990; Austin, 1993), and runs have usually been only a few days or weeks in duration (Rose & Brasseur, 1989; Kaye & Rood, 1989). It seems fair to state that no one approach has proven ideal under all circumstances.

Conventional forward Euler integration can be successfully embedded in multi-D calculations given proper family definitions (Garcia & Solomon, 1983; Kao *et al.*, 1990). The Euler boasts manifold advantages; all concentrations in the chemical time rate of change expressions are known quantities, so that solutions can be obtained directly and cheaply. Furthermore, mass conservation is easily established because cancellations among kinetic terms are obvious (Turco & Whitten, 1974; Rosenbaum, 1976;

*Present address: Earth and Environmental Sciences Division, Geoanalysis Branch, Los Alamos National Laboratories, Los Alamos, New Mexico, U.S.A.

Shimlazaki, 1985). This numerical streamlining, however, is also a property of forward single step differences as a class, and several researchers have pointed out that it could be preserved in situations which would otherwise be destabilizing if projections of future concentrations were used to adjust the knowns (e.g. Turco & Whitten, 1974, 1977). The notion is closely associated with, but not identical to, certain photochemical predictor-correctors (Solomon, 1981; Chang *et al.*, 1987). Our goal in the present work is to explore the potential for family projection/forward differencing to facilitate the conjunction of photochemistry and atmospheric transport. Performance tests are reported for the hybrid scheme within box models of a typical environmental chemical system consisting of well over 100 reactions. Accuracy is achieved at an order of magnitude beyond the tracer time constants, and our programs are found efficient enough to justify computations on massive grids.

We begin the discussion by placing our numerical composites in a fuller historical perspective. A brief chronology is given for the integration of photochemistry within tracer transport codes, with emphasis on the concepts underlying our experiments. Next, the development of our box chemistry is described. Essentially, calculations were conducted in the familiar lower stratosphere in order to establish a baseline, and the time step augmented systematically to reveal potentially unstable entities. Two different projection types were examined: an exponential growth/decay for standard family partitioning, and a linearized implicit version which is appropriate for species ratios fluctuating over a time step. Accuracy is evaluated by breaking the families down and rerunning at higher time resolution. Comparisons between short and long Δt runs are quite encouraging, but we note that they depend on some special contingencies; photolysis rates must be calculated carefully. Finally, the speed of our algorithm is gauged through a series of timing runs. As an incidental, some refinements are listed which should improve code specifications. For example, the variable partitioning projection can be fit into a linear algebraic format which lends itself to automation in setup and alteration of the chemistry.

BACKGROUND

The coupled ordinary differential equations (ODEs) of chemical kinetics can be expressed in many symbolic forms (Widhopf & Victoria, 1973; Turco & Whitten, 1977; Wofsy, 1978; McRae *et al.*, 1982), but for our purposes it is suitable to write

$$ds_i/dt = P_i(s_j) - L_i(s_j) = f_i(s_j) \tag{1}$$

where i and j can vary over all constituent species s. In vector notation,

$$d\mathbf{s}/dt = \mathbf{f}(\mathbf{s}). \tag{2}$$

Deletion of any dynamics operators here can be rationalized as conceptual time splitting. Real use of splitting techniques is becoming more frequent as a means of organizing high dimensionality tracer models (e.g. Oran & Young, 1977; McRae *et al.*, 1982; Penner *et al.*, 1991). Production **P** and loss **L** will be sets of rate expressions which are highly nonlinear because they contain bimolecular terms such as $ks_js_{j'}$, with k signifying a rate constant. It will also generally be true that first order characteristic loss times vary greatly, so that full explicit integration could only be conducted at $\Delta t < s_i/L_i(s_j)$ and might be inconvenient for longer lived species. The latter is one crucial manifestation of the stiffness problem. An instructive rough correspondence links the spectra of constituent loss constants and of eigenvalue reciprocals λ^{-1} derived from the eigen equation $\mathbf{Jx} = \lambda\mathbf{x}$, where **J** designates the Jacobian matrix $\partial\mathbf{f}/\partial\mathbf{s}$ (Liniger & Willoughby, 1970; McRae *et al.*, 1982).

Many atmospheric modeling groups have solved equations (1) and (2) by maintaining all molecules as individual entities. Early low dimensionality studies employed the method of lines (Liskovets, 1965), converting partials into ODEs and then integrating through a Gear routine (Chang *et al.*, 1973; Wuebbles & Chang, 1975) or some exponential fitting algorithm (Liniger & Willoughby, 1970; Thompson & Cicerone, 1982; Cicerone *et al.*, 1983). Both local (Wofsy, 1978; Logan *et al.*, 1978) and partial differential chemistries (Miller *et al.*, 1980, 1981) have been managed at larger time step by placing (2) in its fully implicit finite differencing form

$$\mathbf{s}^{t+1} - \mathbf{s}^t = \mathbf{f}(\mathbf{s}^{t+1})\Delta t \tag{3}$$

in order to foster stability, and then iterating to convergence in a Newton Raphson. The superscript t in this case represents the existent index on the time grid. Any differencing of the form $\mathbf{s}^{t+1} - \mathbf{s}^t = \mathbf{f}\Delta t$ containing a unified concentration vector in **f** will conserve mass because common interspecific terms then cancel (Turco & Whitten, 1974; Shimazaki, 1985), and equation (3) meets this criterion along with the forward Euler. Newton iterations, however, may be quite taxing computationally (McRae *et al.*, 1982). Time can also be advanced semi-implicitly through linearization. In the fastest semi-implicit construction,

$$s_i^{t+1} - s_i^t = [P_i(s_j^t) - s_i^{t+1}/\tau_i]\Delta t; \quad \tau_i = s_i^t/L_i(s_j^t), \tag{4}$$

species are completely decoupled from one another. For a single dimension (Richtmyer, 1957) or multiple dimensions with integration in alternating directions (Peaceman & Rachford, 1955; Brasseur *et al.*, 1990), discrete solutions to the partials can be tridiagonal (Richtmyer, 1957; Brasseur *et al.*, 1990). Concentrations are not evaluated at a single temporal grid point in equation (4), however, and so mass is only balanced for low Δt (Shimazaki & Laird, 1970; Turco & Whitten, 1974, 1977; Shimazaki, 1985; Kaye & Rood, 1989). In a related technique, equation (2) can

be species segregated if it is rewritten as

$$ds_i/dt = P_i(s_j^t) - s_i/\tau_i. \quad (5)$$

Analytical solution then gives the standard exponential growth and decay (Hesstvedt *et al.*, 1978; McRae *et al.*, 1982)

$$s_i^{t+1} = s_i^t \exp(-\Delta t/\tau_i) + P_i(s_j^t)\tau_i[1 - \exp(-\Delta t/\tau_i)]. \quad (6)$$

In multi-species solutions with equation (6), mass conservation has on occasion been verified by calibrations against an integration of known accuracy (Rosenbaum, 1976; Hesstvedt *et al.*, 1978; Isaksen *et al.*, 1978). More elaborate linearizations involving substitution of the Taylor series expansion

$$\mathbf{f}(\mathbf{s}^{t+1}) \cong \mathbf{f}(\mathbf{s}^t) + \mathbf{J}^t\Delta\mathbf{s}, \ \Delta\mathbf{s} = \mathbf{s}^{t+1} - \mathbf{s}^t \quad (7)$$

into equation (3) have been adopted with some success in order to advance in time (Briley & McDonald, 1980; Kasting, 1985; Kasting & Singh, 1986). These appear to be mass balancing, but may not guarantee positive definiteness. Turco *et al.* (1979) have shown that an abbreviated but semi-equivalent substitution into the equations of (1),

$$s_j^{t+1}s_{j'}^{t+1} \cong (s_j^t s_{j'}^{t+1} + s_j^{t+1}s_{j'}^t)/2, \quad (8)$$

for which atom conservation is easily verified, has valuable stabilizing properties.

Numerics which strive to remove short-lived molecules altogether are generally categorized under the banners "steady state" or "photochemical equilibrium", but there are distinct variations on the theme. In one of the more systematic approaches, equation (1) is set equal to zero for constituents with first order loss times below some threshold (McRae *et al.*, 1982; Kasting & Singh, 1986; Brasseur *et al.*, 1990). Mass could become unbalanced if time rates of change are not arranged carefully and completely (Emanuel, 1967; Snow, 1967; Edelson, 1973), but cross checking is usually difficult in the literature. Zeroing of chemical derivatives effectively treats fleeting substances as fixed system parameters rather than tracers. The family method, on the other hand, recognizes that rapidly interchanging species act in concert as persistent constituents in many photochemical situations, then assumes steady state to repartition (Chapman, 1930; Crutzen, 1971; Turco & Whitten, 1974, 1977; Brasseur & Solomon, 1984). A new array of tracers c_n is defined which consists of sums over subsets of $\mathbf{s}$; $c_n = \Sigma_j s_{j,n}$, where j, n denotes molecule j within assemblage n. Species containing more than one atom of a type must of course be weighted accordingly (Turco & Whitten, 1974). For example, Cl_2O_2 may comprise two units of chlorine oxide. Weighting factors will be subsumed here to prevent the notation from becoming too cumbersome. Family scale versions of equations (1)–(7) can then be formulated, with both n and m varying over all groups, as in

$$dc_n/dt = P_n(s_{j,m}) - L_n(s_{j,m}) = f_n(s_{j,m}), \quad (1a)$$

$$d\mathbf{c}/dt = \mathbf{f}(\mathbf{s}), \quad (2a)$$

$$\mathbf{c}^{t+1} - \mathbf{c}^t = \mathbf{f}(\mathbf{s}^{t+1})\Delta t, \quad (3a)$$

$$c_n^{t+1} - c_n^t = [P_n(s_{j,m}^t) - c_n^{t+1}/\tau_n]\,\Delta t; \quad \tau_n = c_n^t/L_n(s_{j,m}^t), \quad (4a)$$

$$c_n^{t+1} = c_n^t \exp(-\Delta t/\tau_n) + P_n(s_{j,m}^t)\tau_n[1 - \exp(-\Delta t/\tau_n). \quad (6a)$$

Analogous statements regarding linearity, solution efficiency, positive definiteness, stability and atom balance remain in force. Identification of appropriate membership j, n can be based on more accurate schemes (Graedel, 1977; Farrow & Graedel, 1977) or on experience (Turco & Whitten, 1977; Solomon & Crutzen, 1981; Garcia & Solomon, 1983) with later confirmation (Solomon, 1981; Chang *et al.*, 1987).

Families have enabled marching at convenient step sizes in a host of detailed 1-D photochemical models (e.g. Crutzen, 1971; Turco & Whitten, 1977; Crutzen *et al.*, 1978), and thus far seem to be a method of choice in higher dimensionality as well (e.g. Garcia & Solomon, 1983; Gidel *et al.*, 1983; Kaye & Rood, 1989: Rose & Brasseur, 1989). Some provisos must be mentioned, however. In 3-D some researchers have minimized the tracer number by eliminating source molecules such as N_2O and the chlorofluorocarbons, which do not contribute significantly to chemistry on short time scales (Kaye & Rood, 1989; Rose & Brasseur, 1989). Additionally, species normally thought of as reservoirs, including $ClONO_2$, N_2O_5, HNO_3, and HCl, tend to be lumped together into stable expanded families in order to promote time step increases (Douglass *et al.*, 1989; Brasseur *et al.*, 1990; Austin, 1993). Rapidly removed constituents then go untransported (Rose & Brasseur, 1989; Brasseur *et al.*, 1990). These approximations are to an extent symptoms of the computational stress imposed by massive grids.

Numerical prediction and correction have played a quality control role in some family modeling investigations. Turco & Whitten (1974) applied equation (4) to individual species to produce $\mathbf{s}^{t+1}$ designed to stabilize equation (3a). Solomon (1981) describes explicit calculation of an initial family vector, partitioning into $\mathbf{s}^{t+1}$ and then averaging of production and loss over t to $t + 1$ before advancing the solution. Chang *et al.* (1987) utilize an affiliated procedure but with the exponential in equation (6a). The present work builds on this predictive philosophy and necessarily shares features with the above, but the overall effect is distinct in critical areas. For example, unlike Solomon (1981) but in common with Chang *et al.* (1987), we insist on initial guesses for family levels which are positive definite and so do not constrain Δt. Unlike Chang *et al.* (1987), but in common with Turco & Whitten (1974), we overlay mass conservation through a second phase of integration with

simple forward differencing and self-consistent $s_{j,m}$. A unified species vector is deduced which will reproduce the estimates in the customized single step

$$\mathbf{c}^{t+1} - \mathbf{c}^{t} = \mathbf{f}(\bar{s})\Delta t. \quad (9)$$

Unlike Turco & Whitten (1974), we project entire families, and our motivation is to expedite chemical calculations in three dimensions.

DEVELOPMENT OF THE PHOTOCHEMICAL PROJECTION SCHEMES

We have chosen to conduct our first tests of these concepts in a rather familiar segment of the atmosphere—the mid-latitude stratosphere. Dozens of modeling studies have centered on this area since the discovery in the early 1970s that anthropogenic input of nitrogen oxides and the chlorofluorocarbons can release radicals which catalytically destroy ozone (see Brasseur & Solomon, 1984; McElroy & Salawitch, 1989). Both *in situ* and remote measurements are also available for crucial trace constituents (Farmer *et al.*, 1976; Anderson, 1977; Ridley *et al.*, 1977; Gille *et al.*, 1980). Although eventually we are hoping to move our photochemical programs into the troposphere, chemistry above the tropopause is for the moment more thoroughly understood on a relative basis. It also happens that a running 1-D code spanning the 10–90 km regime has been available as a template in constructing our box models (Turco & Whitten, 1977; Turco, 1985). The stratosphere thus provides us with an ideal numerical laboratory for our experiments.

Wavelength binning and other model details closely match those in investigations such as Turco (1985), with significant exceptions only in radiative transfer routines; incident photon intensity was attenuated through pure Beer's law absorption in a spherical geometry. Rate constants and cross sections were updated to reflect the latest tabulations (DeMore *et al.*, 1990), and several ozone hole relevant species and reactions have also been included for the sake of currency (e.g. Solomon, 1988; Jones *et al.*, 1989). In particular, chlorine chemistry is supplemented by OClO and by the ClO dimer. All of the calculations were pinned at 45°N latitude. We will focus on the original set, from 20 km in the lower stratosphere, and only outline extensions to higher altitudes briefly, although complete analyses were conducted through 50 km. Concentrations for source and reservoir molecules were initialized from 1-D steady states (Turco & Whitten, 1977; Turco, 1985). All runs began on the vernal equinox and continued for 120 h, through 5 diurnal cycles.

Families were defined at the outset according to standard recipes for 1- and 2-D stratospheres as summarized by Brasseur and Solomon (1984), Shimazaki (1985), and many earlier sources (e.g. Crutzen, 1971; Gidel *et al.*, 1983). Our final choices are listed in Table 1. The system has a natural time constant of roughly a few minutes (Shimazaki, 1985),

Table 1. Stratospheric family definitions for developmental, 3600 s and 0.1–1 s calculations. Actual tracers are indicated in **bold** face, and constituent family memberships are parenthetical. Species containing two atoms of a major atom type are counted twice in overall budgeting; e.g. $Cl_2O_2 = 2ClOx$

100–3600 s	**Ox** (O_3, $O(^3P)$, $O(^1D)$), **H_2O**, **HOx** (HO_2, OH, H), **H_2O_2**, **N_2O**, **NOx** (NO, NO_2, NO_3), **N_2O_5**, **HNO_3**, **HO_2NO_2**, **CH_3Cl**, **CCl_4**, **$CFCl_3$**, **CF_2Cl_2**, **ClOx** (Cl, ClO, ClO_2, HOCl, OClO, Cl_2O_2, Cl_2), **HCl**, **$ClONO_2$**, **CH_4**, **CH_3Ox** (CH_3O_2, CH_3O), **CH_3O_2H**, **CH_2O** (CH_2O, CHO), **CO**, **CO_2**, **CH_3Br**, **BrOx** (Br, BrO, $BrONO_2$, HOBr), **HBr**
0.1 and 1.0 s	**Ox** (O_3, $O(^3P)$, $O(^1D)$), **H_2O**, **HO_2** (HO_2, H), **OH**, **H_2O_2**, **N_2O**, **NO**, **NO_2**, **NO_3**, **N_2O_5**, **HNO_3**, **HO_2NO_2**, **CH_3Cl**, **CCl_4**, **$CFCl_3$**, **CF_2Cl_2**, **ClOx** (Cl, ClO, ClO_2), **HOCl**, **OClO**, **Cl_2O_2**, **Cl_2**, **HCl**, **$ClONO_2$**, **CH_4**, **CH_3Ox** (CH_3O_2, CH_3O), **CH_3O_2H**, **CH_2O** (CH_2O, CHO), **CO**, **CO_2**, **CH_3Br**, **BrOx** (Br, BrO), **$BrONO_2$**, **HOBr**, **HBr**

and so we performed shakedown calculations in the forward Euler mode at $\Delta t = 100$ s. The time step was then raised in 100-s increments until irregularities became apparent. Because our program zeroes negative concentrations in order to avoid complex arithmetic, instabilities usually manifested themselves as crashes within diurnal profiles. The first problems arose at 600 s in the methane derivative and odd hydrogen families. In Fig. 1, for example, the expected diurnal cycling is almost established on the equinox, but does not recover on subsequent days. When the procedures described below are inserted, negative concentrations are avoided entirely and so do not affect our ultimate answers.

Partitioning of the individual species in many families is determined largely by interactions with slowly varying entities, and so can be considered constant over the time steps dealt with here. Distribution of hydrogen atoms between HO_2 and OH, for example, is controlled mainly by reactions with ozone in the lower to middle stratosphere (Brasseur & Solomon, 1984). We have paired the projection and

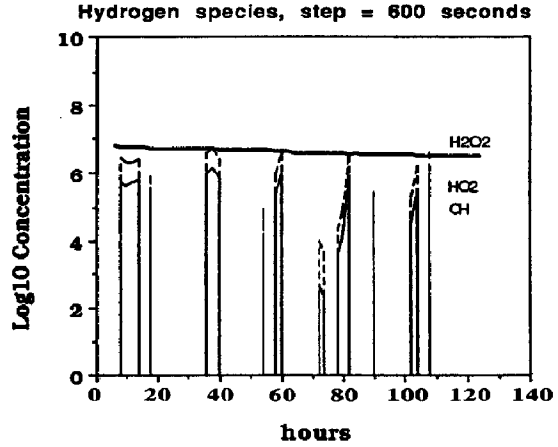

Fig. 1. Members of the hydrogen oxide families modeled at 600 s time step without projection. Five diurnal cycles are plotted for 45°N latitude and 20 km, beginning on the vernal equinox. The vertical axis has units of log concentration, with concentration in molecules cm^{-3}.

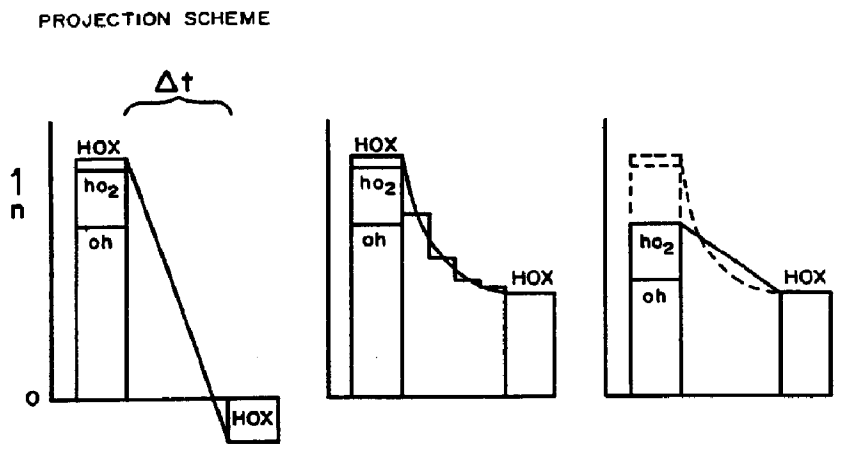

Fig. 2. Schematic diagram of the projection scheme introduced to stabilize the odd hydrogen family and others for which partitioning is constant over the time step. First panel: increases in step size lead to instabilities, the pathological extreme being negative concentrations. Second panel: the problem could be handled by lowering Δt. Third panel: alternatively, species concentrations can be adjusted to produce a pre-determined stable, accurate and positive definite value.

stabilization process whenever possible by calculating a single set of partitioning ratios $R_j(s)$ at time t, and holding them through $t + 1$. The erratic HOx behavior in Fig. 1 stems fundamentally from the relationship $\tau(\mathrm{HO}x) < \Delta t = 600$ s, together with use of the Euler. Although semi-implicit differencing would also yield non-negative concentrations, we have the program perform initial HOx and $\mathrm{CH_3O}x$ c^{t+1} estimates in the more accurate exponential growth and decay equation (6a). The species concentrations actually sent to time step advance are adjusted to aim for these values by solving

$$c_n^{t+1} - c_n^t = [P_n(s_{j,m}^t) - L_n(s_{j,m}^t, \bar{s}_{j,n})]\Delta t \qquad (10)$$

for $\bar{s}_{j,n}$. For families with first order losses only, the overbar concentrations derived in this fashion are in fact integrated averages over Δt. To improve consistency in the series (6a) then (10), $s_{j,m}^t$ are replaced by $\bar{s}_{j,m}$ while moving from one projected family to the next. The cycle over n is of course repeatable, but we have attempted to avoid iterations. The projection is completed with full mass balance when $\bar{s}_{j,n}$ are sent as a unit to equation (9) for time stepping. The constant partitioning method is illustrated schematically for odd hydrogen in Fig. 2, and a snapshot of the result is offered as Fig. 3. Cigar shaped daily profiles observed at lower time step are restored.

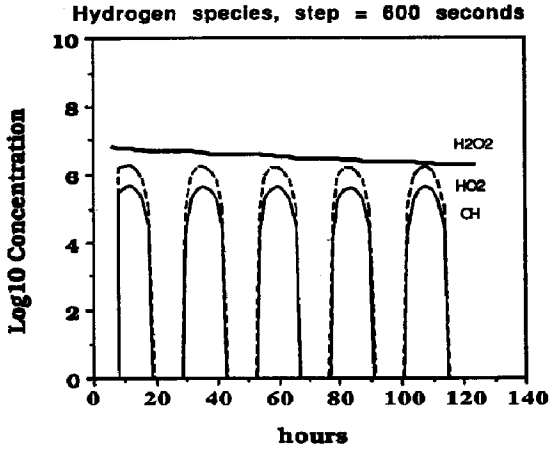

Fig. 3. Members of the hydrogen oxide families modeled at 600 s time step with projection. Five diurnal cycles are plotted for 45°N latitude and 20 km, beginning on the vernal equinox. The vertical axis has units of log concentration, with concentration in molecules cm^{-3}.

The active chlorine family labeled ClOx in Table 1 has been defined on the basis of photochemical equilibrium at local noon as a test case in nonconstant partitioning. Long-lived major reservoirs HCl and $\mathrm{ClONO_2}$ are not incorporated, so that the better chemical resolutions achieved in low dimensionality are approached (e.g. Solomon & Garcia, 1984). The grouping does include the mid-latitude night time reservoir HOCl and its high latitude cousins OClO and $\mathrm{Cl_2O_2}$, however, and because they are removed only through photolysis, they should detach kinetically at dusk. As shown in Fig. 4, constant partitioning ratios can suppress the night reservoir concentrations artificially after dark. Turco & Whitten (1974) have pointed out that species partitioning calculated implicitly within the family holds the potential to reflect time dependent $R_j(s)$, and other studies have touched upon the subtlety (Gidel *et al.*, 1983; Kaye & Rood, 1989). If the implicit integrations are performed in a coupled algebraic sense, then mass can be conserved. Moreover, $t + 1$ concentrations from equation (3) already constitute the averages needed to force stable answers from equation (9), as can readily be verified by summing over $\mathrm{d}s_{j,n}/\mathrm{d}t$ within n. A family internal integration can thus function as a partition and a projection simultaneously. Accordingly, we have set up our

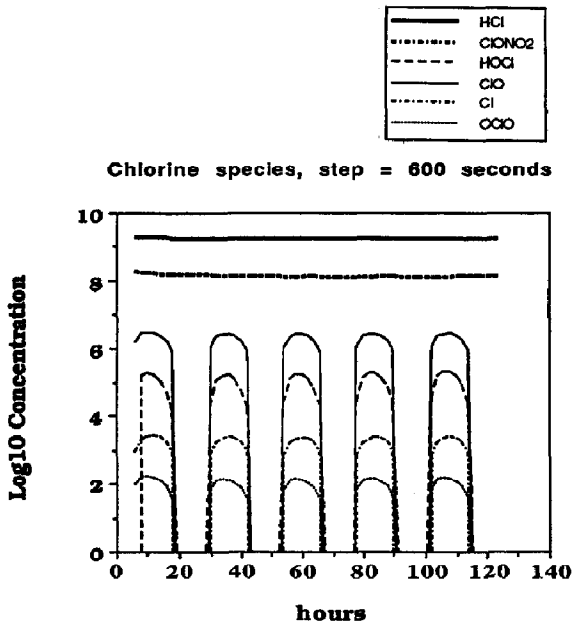

Fig. 4. Chlorine containing species modeled at 600 s time step with projection, but also with constant partitioning. Five diurnal cycles are plotted for 45°N latitude and 20 km, beginning on the vernal equinox. The vertical axis has units of log concentration, with concentration in molecules cm^{-3}.

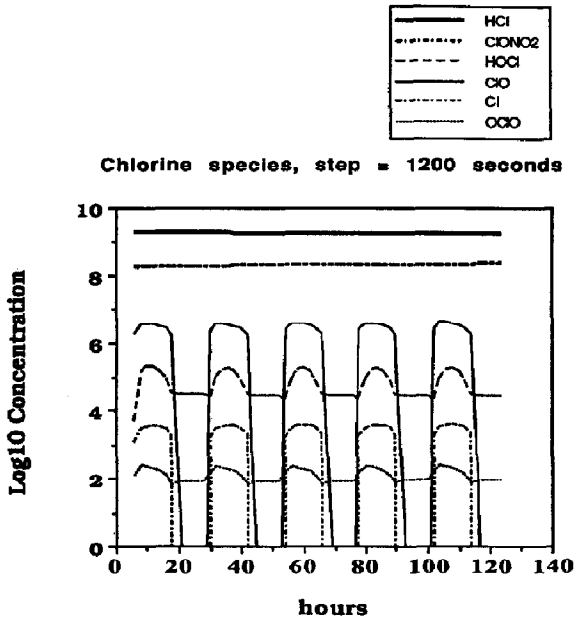

Fig. 6. Chlorine containing species modeled at 1200 s time step with a linearized implicit partition/projection. Five diurnal cycles are plotted for 45°N latitude and 20 km, beginning on the vernal equinox. The vertical axis has units of log concentration, with concentration in molecules cm^{-3}.

active chlorine calculations in the spirit of equation (3). The critical reactants are extra-familial, so that most terms are linear by default. Chlorine monoxide self-reaction is linearized according to equation (8), which produces a positive definite form because $j = j'$. The $s^{t+1}_{j,\mathrm{ClO}x}$ immediately become $\bar{s}_{j,\mathrm{ClO}x}$, and are sent to equation (9) along with values from other m. The family internal and linear implicit projection technique is illustrated schematically in Fig. 5, and the outcome is plotted in Fig. 6. Night time reservoirs reappear along with changes in the partitioning ratios.

The time step was raised slowly at 20 km, and constant partitioning projections were inserted as necessary, until the box model could be run with complete stability at Δt 3600 s, an order of magnitude above time constants for the stiffest tracers HOx and CH_3Ox. The box was then moved vertically through the stratosphere at constant latitude in 10 km jumps, and the entire procedure repeated at each altitude up

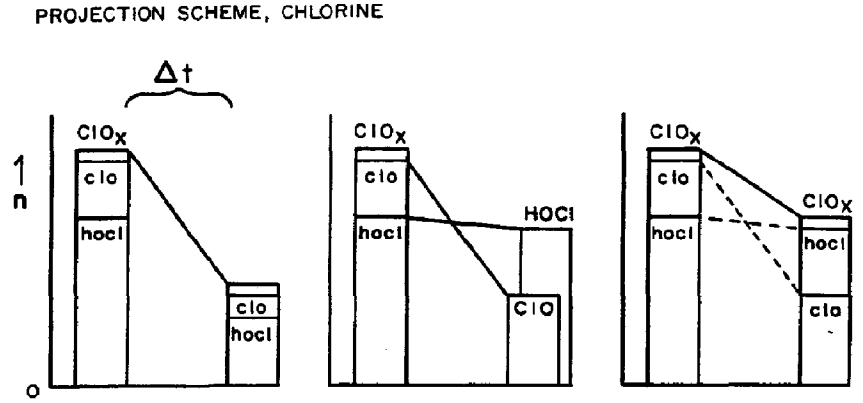

Fig. 5. Schematic diagram of a linearized implicit projection scheme permitting kinetic detachment of night time reservoirs from the active chlorine family. First panel: increases in time step lead to inaccuracies if constant partitioning is assumed, and in particular, low reservoir concentrations during dark periods. Second panel: the problem could be handled by defining the night time reservoirs as separate tracers. Third panel: alternatively, implicit projections reflect decoupling as necessary if some species become long lived.

to 50 km inclusive. Predictions were implemented for each of the families $ClONO_2$, N_2O_5, HOx, CH_3Ox, and CH_2O, and the halogen oxides were partitioned implicitly. In the final coding version used on the calculations in the remainder of the text, all these tracers were projected together.

ACCURACY TESTING

The profiles displayed in Figs 1–6 parallel published diurnal cycles from models conducted over the last two decades (Whitten & Turco, 1974; Ogawa Shimazaki, 1975; Crutzen *et al.*, 1978), so that gross features of the chemistry are clearly correct in at least a rough sense. Because the present study represents the development phase in a new blending of chemical numerics, a more strenuous assessment of accuracy would also seem to be in order. We base our analysis here on comparison with calibration runs supporting an identical list of chemical reactions, but smaller family units (Solomon, 1981; Douglass *et al.*, 1989; Jacob *et al.*, 1989; Austin, 1993). In fact, we have dissected our groupings until virtually the only species not treated as individual tracers are the atoms. The calibration configuration is given in the lower half of Table 1. A baseline for accuracy was established by running the individual species over the usual 5 days at 1.0 and 0.1 s time steps. All concentrations matched to within one part in 10^4 except during the hours containing sunrise and sunset, when the agreement occasionally fell to one part in 10^3; the two sets of low step size results are thus nearly identical. Further evidence for their realism could be gained from runs against a code of known accuracy. It might also be possible in some instances to formalize error limits for complex numerics analytically (Engquist *et al.*, 1978; Briley & McDonald, 1980).

After similarity was established for the 0.1 and 1.0 s time developments, 1.0 s concentrations for all species

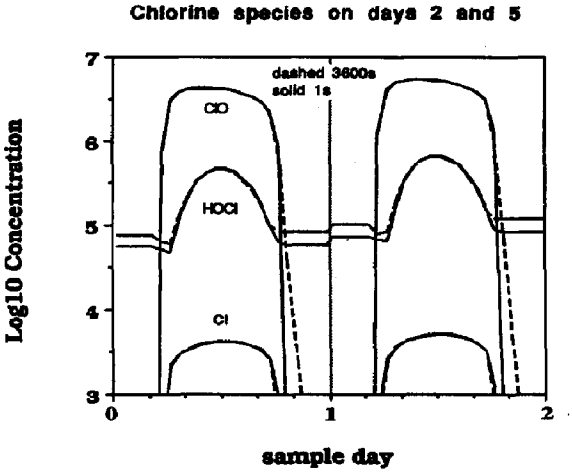

Fig. 8. A comparison of 3600 s and 1 s integrations for some active chlorine species, on the second and fifth days. The vertical axis has units of log concentration, with concentration in molecules cm^{-3}.

were integrated and averaged over each hour, and then plotted on the half hour along with the 3600 s results. Species comparisons comprise a more severe test for chemical exactness because the families are by definition longer lived and easier to track. A typical level of agreement for a projected family is illustrated for HOx in Fig. 7. The 1 s and 1 h concentrations fall within one part in 10^2 during most of the daylight hours, and within 10% during the hours bracketing dawn and dusk. With a few exceptions to be noted below, accuracies for source and reservoir species were better than 1% 24 h per day.

Figure 8 overlays long and short time step calculations for several members of the active chlorine family. The implicitness of the family internal partition/projection leads to the usual lag on the decay

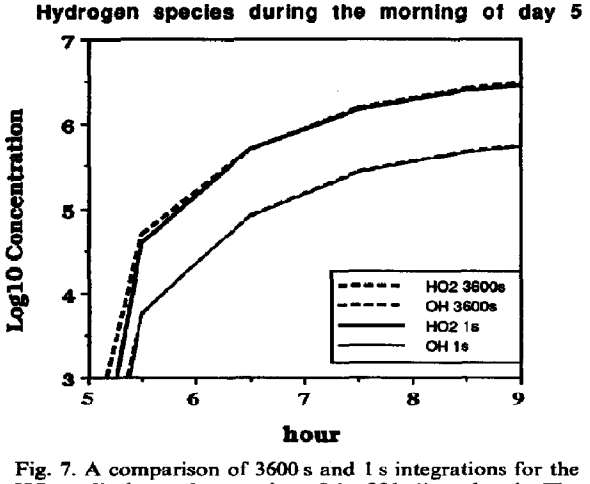

Fig. 7. A comparison of 3600 s and 1 s integrations for the HOx radicals, on the morning of the fifth diurnal cycle. The vertical axis has units of log concentration, with concentration in molecules cm^{-3}.

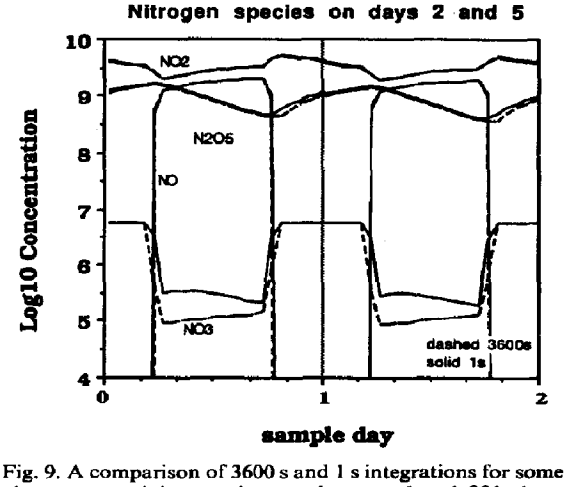

Fig. 9. A comparison of 3600 s and 1 s integrations for some nitrogen containing species, on the second and fifth days. The vertical axis has units of log concentration, with concentration in molecules cm^{-3}.

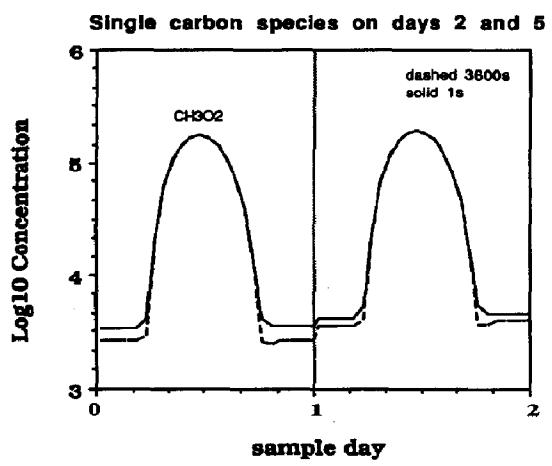

Fig. 10. A comparison of 3600 s and 1 s integrations for the methyl peroxy radical, the predominant member of the methane oxidation products family, on the second and fifth days. The vertical axis has units of log concentration, with concentration in molecules cm^{-3}.

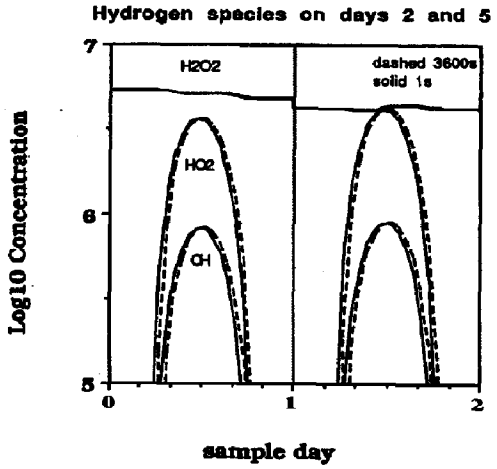

Fig. 11. A comparison of 3600 s and 1 s integrations for the odd hydrogen components HO_2 and OH on the second and fifth days, with photolysis constants calculated at the beginning of each time step. The vertical axis has units of log concentration, with concentration in molecules cm^{-3}.

side for both ClO and HOCl. This can be thought of as the numerical price to be paid for variable species to family ratios. The matches are satisfying on the whole for nitrogen species (Fig. 9), but the 1 h runs come up a factor of two short on NO_3 during the daytime. We have determined that the deficiency lies in the standard NO*x* partitioning we have adopted, and not in the projection numerics. The ratio recipe we utilized does not include photolysis of N_2O_5 as an NO_3 source. Clearly, the potential for error exists even in programming of the algebra behind partitioning. Another family related problem was encountered within the methane derivatives and is plotted as Fig. 10. In this case the 1 h calculations overshoot removal at dusk. The major CH_3O_2 loss is via reaction with NO, which is over approximated somewhat as the sun sets due to constancy of the partitioning in NO*x*.

PHOTOLYSIS RATES

Temperature fluctuations are small enough in the stratosphere that the kinetic rate constants are generally assumed invariant over a time step. Photolysis rates *J*, however, can alter dramatically near sunrise and sunset, and one by-product of our program development has been the identification of some photolytic pitfalls which accompany long time step calculations. As a start up expedient, we began our investigations with *J* values calculated at time *t*. Comparisons with the short time step runs revealed, however, that this procedure produced a phase shift for some radical families. The shift is illustrated for the odd hydrogen species in Fig. 11. At the 1 h step size, HO_2 and OH concentrations are late in both rising and falling. The explanation traces to photolysis; on the equinox and for a few days thereafter, the sun rises at just before 6 a.m. and sets at just past 6 p.m. in the lower stratosphere. High resolution integrations pick up the extra energy input in the morning, while low resolution artificially extends photoreaction in the evening. Our first repair involved centering *J* computations on the half hour, but this introduced new problems. As shown for the oxygen atoms in Fig. 12, the phase shift was eliminated in that short lived species peaked at local noon, but the 3600 s concentrations now dropped early at dusk on the equinox. In the $J(t + 1/2)$ case, the long time step calculations could miss energy inputs on both sides of the daylight period. The inaccuracies had righted themselves by day 5 because of an increase in the day length moving into spring.

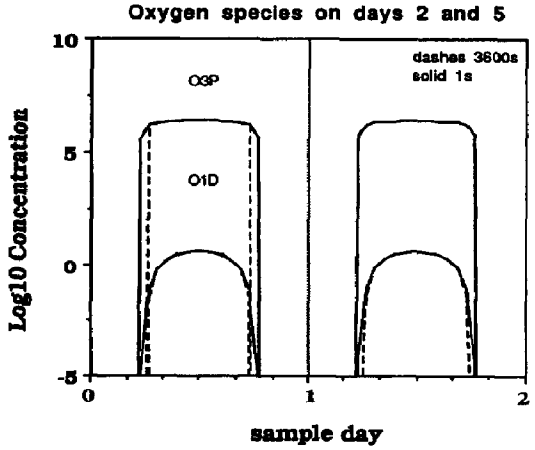

Fig. 12. A comparison of 3600 s and 1 s integrations for the oxygen atoms on the second and fifth days, with photolysis constants calculated on the half hour. The vertical axis has units of log concentration, with concentration in molecules cm^{-3}.

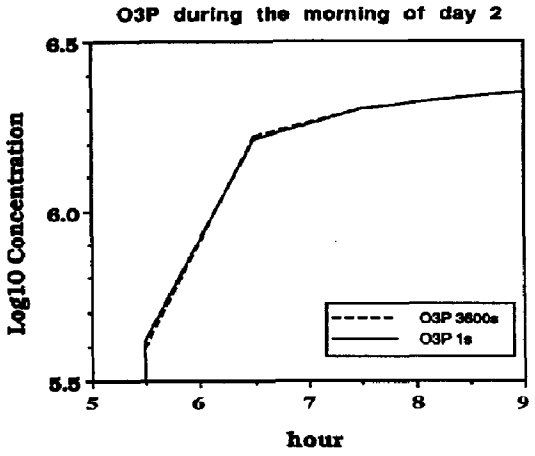

Fig. 13. A comparison of 3600 s and 1 s integrations for the oxygen atom on the morning of the second day, with photolysis constants integrated and averaged over the longer time step. The vertical axis has units of log concentration, with concentration in molecules cm^{-3}.

Discrepancies stemming from the exact placement of photolyses were ultimately eased by averaging J values over the 1 h time steps. In the present work we have performed the calculation

$$\bar{J} = \left(\int_t^{t+1} J(t)\, dt \right) / \Delta t \qquad (11)$$

by merely dividing Δt into a finite number of evenly spaced intervals, and we have made a rough attempt to minimize the expense of the photolytic routines by restricting the procedure to hours embracing sunrise and sunset. Typical results have already been provided as Figs 7–10, and Fig. 13 zooms on a portion of the second day for the oxygen atom. Species produced by photolysis of sources in the optically thick 300 nm region of the spectrum may experience effective sunrise later in the morning, with attendant disparities in the 6 a.m. to 7 a.m. time slot. The $O(^1D)$ atom exhibits this behavior in Fig. 14. Averaging of photolysis rates could be pushed beyond sunrise to ameliorate the problem, and we are presently at work on parameterized radiation coding to render more frequent J calculations affordable.

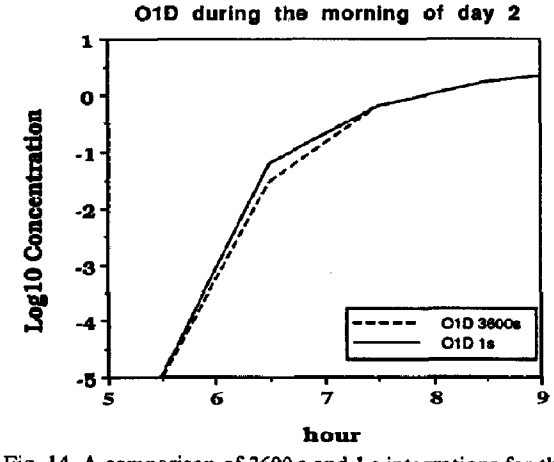

Fig. 14. A comparison of 3600 s and 1 s integrations for the $O(^1D)$ atom on the morning of the second day, with photolysis constants integrated and averaged over the longer time steps when they bracket dawn or dusk. The vertical axis has units of log concentration, with concentration in molecules cm^{-3}.

DISCUSSION

We have argued thus far that the sequence of accurate projections followed by the adjusted, Euler-like forward advance in equation (9) enables an increase of time steps well above the lifetimes of the stiffest family tracers, and does so with mass conservation. Both the projection and family partitioning processes, however, entail a certain amount of computational overhead. The real intention of our studies has been the design of detailed photochemical routines for merging with 3-D tracer transport codes and/or general circulation models, and so we have also monitored the tractability of operating our package at high dimensionality through a series of CPU timing tests on a Cray YMP. The purely chemical subroutines consumed most of the processing time, and they in turn were dominated by the predictive and diagnostic family calculations. A single 1 h time step in the box mode required roughly 10^{-4} s. Extrapolation to a hypothetical 3-D grid with $100 \times 100 \times 10$ compartments suggests that an atmospheric year of kinetics at our complexity level could be successfully modeled in on the order of hours of clock time. We conclude that our projection/forward numerics merit testing with GCM wind fields.

Figure 15 capsulizes some of the overhead issues relevant to multi-dimensional photochemistry programs, and is useful in placing the potential of our method into perspective. The number of operations required to finish pure chemistry subsections during one time step is plotted logarithmically against concentration vector size. The operation levels shown are approximate in several ways. In the interest of simplicity, for example, we have restricted our counting to multiplications because they tend to dominate computational expense if distributed evenly with addition or subtraction. The partition/projection and feasibility bands are fixed solely from the experiences outlined in the present work. Two common finite differencing molecules which employ a unified concentration vector within kinetic terms are graphed as the solid curves. Even if it is linearized, the implicit equation (3) requires some type of matrix inversion with $\sim n^3/3$ multiplications (Oran & Boris, 1981), and costs escalate rapidly as the number of tracers rises. The implicit function in the figure in fact represents a lower limit, since accuracy is lost without iteration to convergence. The forward advance in equation (9), on the other hand, is extremely cheap in and of itself. Partitioning recipes and our projection

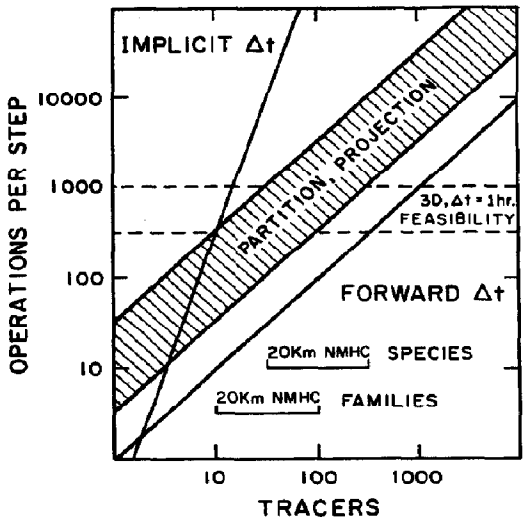

Fig. 15. Approximate computational overhead associated with several types of chemical numerics, expressed in units of multiplicative operations per time step as a function of the total number of tracers. The label Implicit refers to equations such as (3), which can be linearized for approximate or iterative solution. Forward signifies differencing as in equation (9). Typical family and species ranges in several atmospheric situations are indicated as the horizontal bars. 20 km designates stratospheric photochemistry. NMHC is a standard abbreviation for the nonmethane hydrocarbons. The influence of their oxidation on tropospheric ozone levels is a topic of current debate.

techniques add more than an order of magnitude to the solution, but like the equation (9) integration they scale as n^1. One of our upcoming goals is to apply the procedures developed here to tropospheric organic chemistry, both in the urban environment and in global tropospheric ozone/nonmethane hydrocarbon relationships. Organic oxidation intermediates will undoubtedly swell the tracer total, but because of the first power scaling, the chemistry should still be programmable in 3-D.

Projection and partitioning in our stratospheric box model have so far been edited manually for the most part, and are somewhat inflexible to alterations in species and reaction catalogs, or in family definitions. Automation can greatly facilitate changes in chemical input (Edelson, 1976), and should mesh well with the internal implicit predictor polished here on active chlorine species, because intra-familial kinetics are either inherently linear or easily linearizable through substitution [see equation (8)]. Eventually we envision reading in data analogous to Table 1, plus chemical reactions, and then asking the coding itself to build small, individual family matrices for solving equation (3). Inversion would give $R_j(s)$ and bolster stability simultaneously. Because kinetic systems can generally be arranged so that tracers consist of fewer than about 5 species, automation could conceivably lower the number of operations per step, and so lead to efficiency enhancements (Fig. 15). The delays associated with implicit integration would of course translate to some sacrifice in fidelity in this scenario.

SUMMARY

The collection of rapidly exchanging species into family assemblages with reasonable lifetimes has been a major strategy for circumventing stiffness in atmospheric photochemical modeling (Chapman, 1930; Crutzen, 1971; Gidel *et al.*, 1983; Garcia & Solomon, 1983). On multi-dimensional grids families have sometimes been assigned to assure photochemical equilibrium over time steps on the order of the diurnal cycle (Gidel *et al.*, 1983; Brasseur *et al.*, 1990), and radicals or source molecules have sometimes been excluded altogether (Kasting & Singh, 1986; Rose & Brasseur, 1989; Kaye & Rood, 1989; Brasseur *et al.*, 1990). Three-dimensional calculations have also recently been performed on single species or families with much of the photochemistry parameterized off-line (Jacob *et al.*, 1989; Spivakovsky *et al.*, 1990). These adjustments are made at least partially in response to computational constraints, but raise questions with regard to accuracy and chemical detail (Douglass *et al.*, 1989; Austin, 1993) as well as mass balance (Emanuel, 1961; Snow, 1967; Edelson, 1973; Hesstvedt *et al.*, 1978).

We have described here as a complementary offering a technique for stabilizing short lived groups as the time step is increased beyond their characteristic constants. In instances for which partitioning ratios do not vary over Δt, stable and positive definite estimates can be made for final family concentrations using a unimolecular exponential growth and decay equation. Atom balancing can then be added by calculating step averaged species concentrations which will reproduce the positive definite result in a forward solver. If constancy of partitioning is not guaranteed, ratios can still be tracked through a linearized, assemblage-internal implicit scheme which mimics forward differencing sufficiently that the step averages do not have to be arrived at separately. Judicious application of the tracer projections followed by forward time advance combines implicit stability with desirable features of the explicit mode—viz. clarity, speed and material conservation.

These concepts were developed in a box model positioned in the mid-latitude stratosphere by initializing with standard family definitions and 1 to 2 min time increments, then moving Δt upward and introducing predictor coding as instabilities were uncovered. An eventual step of 1 h was checked for accuracy by comparison with runs conducted mainly on individual species, at 0.1 and 1.0 s. Agreement was better than one part in 10^2 during most of the daylight period or better than 10% at dawn and dusk for radicals, and exceeded 1% continually for reservoirs, excepting implicit time lags in the decay phase. It became evident during early calculations that integration of photolysis rates is essential in achieving

such comparisons. Extrapolation of CPU timing tests to a hypothetical GCM grid indicates that the combination of positive definite projection with the mass saving forward numerics could be adapted to the simulation of detailed photochemical kinetics in three dimensions.

Late versions of the programs highlighted in this text can be obtained for inspection or assimilation through correspondence with Scott Elliott.

Acknowledgements—The authors wish to thank R. Rood for helpful discussions. This project has been supported by NASA Ames consortium Grants NCA2-305 and 377, NASA Grant NAGW-2183, and NSF Grant ATM89-11836.

REFERENCES

Anderson J. G., Margitan J. J. & Stedman D. H. (1977) *Science* **198,** 501.
Austin J. (1993) *J. Geophys. Res.* In press.
Brasseur G. & Solomon S. (1984) *Aeronomy of the Middle Atmosphere*. D. Reidel, Dordrecht.
Brasseur G., Hitchman M. H., Walters S., Dymek M., Falise E. & Pirre M. (1990) *J. Geophys. Res.* **95,** 5639.
Briley W. R. & McDonald H. (1980) *J. Comput. Phys.* **34,** 54.
Carmichael G. R., Peters L. K. & Kitada T. (1986) *Atmos. Environ.* **20,** 173.
Chang J. S., Hindmarsh A. C. & Madsen N. K. (1973) Simulation of chemical kinetics transport in the stratosphere. In *Stiff Differential Systems* (Edited by Willoughby R. S.). Plenum Press, New York.
Chang J. S., Brost R. A., Isaksen I. S. A., Madronich S., Middleton P., Stockwell W. R. & Walcek C. J. (1987) *J. Geophys. Res.* **92,** 14681.
Chapman S. (1930) *Mem. R. Meteorol. Soc.* **3,** 103.
Cicerone R. J., Walters S. & Liu S. C. (1983) *J. Geophys. Res.* **88,** 3647.
Crutzen P. J. (1971) *J. Geophys. Res.* **76,** 7311.
Crutzen P. J., Isaksen I. S. A. & McAfee J. R. (1978) *J. Geophys. Res.* **83,** 345.
Cunnold D., Alyea F., Phillips N. & Prinn R. (1975) *J. Atmos. Sci.* **32,** 170.
DeMore W. B., Sander S. P., Golden D. M., Molina M. J., Hampson R. F., Kurylo M. J., Howard C. J. & Ravishankara A. R. (1990) *Chemical Kinetics and Photochemical Data for Use in Stratospheric Modeling Evaluation*, Number 9, JPL Publ. 90-1.
Douglass A. R., Jackman C. H. & Stolarski R. S. (1989) *J. Geophys. Res.* **94,** 9862.
Dunker A. M. (1986) *Atmos. Environ.* **20,** 479.
Edelson D. (1973) *J. Comput. Phys.* **11,** 455.
Edelson D. (1976) *Comput. Chem.* **1,** 29.
Emanuel G. (1967) *J. Phys. Chem.* **71,** 1161.
Engquist B., Gustafson B. & Vreeburg J. (1978) *J. Comput. Phys.* **27,** 295.
Farmer C. B., Raper O. F. & Norton R. H. (1976) *Geophys. Res. Lett.* **3,** 13.
Farrow L. A. & Graedel T. E. (1977) *J. Phys. Chem.* **81,** 2480.
Garcia R. R. & Solomon S. (1983) *J. Geophys. Res.* **88,** 1379.
Gear C. W. (1969) *Inf. Process.* **68,** 187.
Gidel L. T., Crutzen P. J. & Fishman J. (1983) *J. Geophys. Res.* **88,** 6622.
Gille J. C., Bailey P. L. & Russell P. L. (1980) *Philos. Trans. R. Soc. London* **296,** 205.
Graedel T. E. (1977) *J. Phys. Chem.* **81,** 2372.
Hesstvedt E., Hov O. & Isaksen I. S. A. (1978) *Int. J. Chem. Kin.* **10,** 971.
Isaksen I. S. A., Hov O. & Hesstvedt E. (1978) *Environ. Sci. Technol.* **12,** 1279.
Jacob D. J., Sillman S., Logan J. A. & Wofsy S. C. (1989) *J. Geophys. Res.* **94,** 8497.
Jones R. J., Austin J., McKenna D. S., Anderson J. G., Fahey D. W., Farmer C. B., Heidt L. E., Kelly K. K., Murphy D. M., Proffitt M. H., Tuck A. F. & Vedder J. F. (1989) *J. Geophys. Res.* **94,** 11529.
Kao C. Y. J., Glatzmaier G. A., Malone R. C. & Turco R. P. (1990) *J. Geophys. Res.* **95,** 22495.
Kasting J. F. (1985) Photochemical consequences of enhanced carbon dioxide levels in earth's early atmosphere. In *The Carbon Cycle and Atmospheric Carbon Dioxide: Natural Variations Archean to Present* (Edited by Sundquist E. T. & Broecker W. S.), Geophysical Monograph 32. American Geophysical Union, Washington, DC.
Kasting J. F. & Singh H. B. (1986) *J. Geophys. Res.* **91,** 13239.
Kasting J. F., Pollack J. B. & Crisp D. (1984) *J. Atmos. Chem.* **1,** 403.
Kaye J. A. & Rood R. B. (1989) *J. Geophys. Res.* **94,** 1057.
Liniger W. & Willoughby R. A. (1970) *SIAM J. Numer. Anal.* **7,** 47.
Liskovets O. A. (1965) *Differential Equations* **1,** 1662.
Logan J. A., Prather M. J., Wofsy S. C. & McElroy M. B. (1978) *Philos. Trans. R. Soc. London Ser. A.* **290,** 187.
Mahlman J. D. & Moxim W. J. (1978) *J. Atmos. Sci.* **35,** 1340.
Marsden A. R., Frenklach M. & Reible D. D. (1987) *J. Air Pollut. Control Assoc.* **37,** 370.
McElroy M. B. & Salawitch R. J. (1989) *Planet. Space Sci.* **37,** 1653.
McRae G. J., Goodin W. R. & Seinfeld J. H. (1982) *J. Comput. Phys.* **45,** 1.
Miller C., Steed J. M., Filkin D. L. & Jesson J. P. (1980) *Nature* **288,** 461.
Miller C., Filkin D. L., Owens A. J., Steed J. M. & Jesson J. P. (1981) *J. Geophys. Res.* **86,** 12039.
Ogawa T. & Shimazaki T. (1975) *J. Geophys. Res.* **80,** 3945.
Oran E. S. & Boris J. P. (1981) *Prog. Energy Combust. Sci.* **7,** 1.
Oran E. S. & Young T. R. (1977) *J. Phys. Chem.* **81,** 2463.
Peaceman D. W. & Rachford H. H. (1955) *J. Soc. Indust. Appl. Math.* **3,** 28.
Penner J. E., Atherton C. S., Dignon J., Ghan S. J. & Walton J. J. (1991) *J. Geophys. Res.* **96,** 959.
Prather M. J., McElroy M. B., Wofsy S. C., Russell G. & Rind D. (1987) *J. Geophys. Res.* **92,** 6579.
Reinhardt W. A. (1977) *J. Phys. Chem.* **81,** 2427.
Richtmyer R. D. (1957) *Difference Methods for Initial Value Problems*. Interscience, New York.
Ridley B. A., McFarland M., Bruin J. T., Schiff H. I. & McConnell J. C. (1977) *An. J. Phys.* **55,** 212.
Rose K. & Brasseur G. (1989) *J. Geophys. Res.* **94,** 16387.
Rosenbaum J. S. (1976) *J. Comput. Phys.* **20,** 259.
Shimazaki T. (1985) *Minor Constituents in the Middle Atmosphere*. Reidel, Dordrecht.
Shimazaki T. & Laird A. R. (1970) *J. Geophys. Res.* **75,** 3221.
Snow R. H. (1967) *J. Phys. Chem.* **71,** 1162.
Solomon S. (1981) One and two dimensional photochemical modeling of the chemical interactions in the middle atmosphere (0–120 km), Ph.D. dissertation, University of California, Berkeley.
Solomon S. (1988) *Rev. Geophys.* **26,** 131.
Solomon S. & Crutzen P. J. (1981) *J. Geophys. Res.* **86,** 1140.
Solomon S. & Garcia R. R. (1984) *J. Geophys. Res.* **89,** 11633.
Spivakovsky C. M., Yevich R., Logan J. A., Wofsy S. C. & McElroy M. B. (1990) *J. Geophys. Res.* **95,** 18441.
Thompson A. M. & Cicerone R. J. (1982) *J. Geophys. Res.* **87,** 8811.

Turco R. P. (1985) The photochemistry of the stratosphere. In *The Photochemistry of Atmospheres* (Edited by Levine J. S.), pp. 77–128, Academic Press, New York.

Turco R. P. & Whitten R. C. (1974) *J. Geophys. Res.* **79**, 3179.

Turco R. P. & Whitten R. C. (1977) *The NASA Ames Research Center One and Two Dimensional Stratospheric Models part 1: the One Dimensional Model*, NASA Tech. Publ. TP-1002.

Turco R. P., Hamill P., Toon O. B., Whitten R. C. & Kiang C. S. (1979) *The NASA Ames Research Center Stratospheric Aerosol Model 1. Physical Processes and Computational Analogs*, NASA Tech. Publ. TP-1362.

Weigert F. J. (1987) *Comput. Chem.* **11**, 273.

Whitten R. C. & Turco R. P. (1974) *J. Geophys. Res.* **79**, 1302.

Widhopf G. F. & Victoria K. J. (1973) *Comput. Fluids* **1**, 159.

Wofsy S. C. (1978) *J. Geophys. Res.* **83**, 364.

Wuebbles D. J. & Chang J. S. (1975) *J. Geophys. Res.* **80**, 2637.